Published in final edited form as:
Ultrasound Obstet Gynecol. 2014 April ; 43(4): 452–458. doi:10.1002/uog.12555.

Shear Wave Speed Estimation in the Human Uterine Cervix

Lindsey C. Carlson[1], **Helen Feltovich**[1,2], **Mark L. Palmeri**[3], **Jeremy J. Dahl**[3], **Alejandro Munoz del Rio**[1], and **Timothy J. Hall**[1]

[1]Medical Physics Department, University of Wisconsin, Madison, WI 53706

[2]Maternal Fetal Medicine Department, Intermountain Healthcare, Provo, Utah

[3]Biomedical Engineering Department, Duke University, Durham, NC

Abstract

Objectives—Our goals were to explore the spatial variability within the cervix and the sensitivity of shear wave speeds (SWS) to assess softness/stiffness differences in ripened (softened) versus unripened tissue.

Methods—We obtained SWS estimates from hysterectomy specimens (n=22), a subset of which were ripened (n = 13). Multiple measurements were made longitudinally along the cervical canal on both the anterior and posterior sides of the cervix. Statistical tests of differences in the proximal vs. distal, anterior vs. posterior, and ripened vs. unripened cervix were performed with individual two-sample t-tests and a linear mixed model.

Results—We discovered that SWS estimates monotonically increase from distal to proximal longitudinally along the cervix, that they also vary in the anterior compared to the posterior cervix, and that they are significantly different in ripened vs. unripened cervical tissue. Specifically, the mid position SWS estimates for the unripened group were 3.45±0.95 m/s (anterior) and 3.56±0.92 m/s (posterior), and 2.11±0.45 m/s (anterior) and 2.68±0.57 m/s (posterior) for the ripened ($p<0.001$).

Conclusions—We propose that shear wave speed estimation may be a valuable research and, ultimately, diagnostic tool for objective quantification of cervical stiffness/softness.

Keywords

cervix; preterm birth; shear wave speeds; ultrasound

INTRODUCTION

Spontaneous preterm birth (sPTB) affects 13 million babies annually.[1] Its incidence would be reduced by only 5% even if all patients received appropriate education and intervention.[2] As stated in The Lancet, “the conclusion that 95% of preterm births are intractable to current therapies suggests that substantial further research is needed.”[2]

The pathophysiological pathways to preterm birth are overlapping and multifactorial, and therefore studying end processes that occur just prior to delivery, such as cervical remodeling, has been proposed as a starting point for targeted exploration of mechanisms.[3–7] Unfortunately, remodeling is complex. The pregnant cervix undergoes four stages facilitated by differential changes in intertwining layers of aligned collagen: (1) initial softening, (2) shortening and marked softening (“ripening”), (3) active dilation, and (4) post-delivery recovery.[8–27] Biopsies reveal microstructural and histologic changes[5;19] but invasive exploration is impractical *in vivo* and results are difficult to interpret because of unrepresentative sampling.[8]

Noninvasive techniques to assess cervical microstructural properties have been recently explored.[28] One of these, elastography, assesses tissue stiffness/softness by evaluating relative deformation between neighboring areas of tissue via comparison of images before and after manual compression.[29–32] Efforts have exposed significant challenges with assessing overall stiffness of the cervix and standardizing the compressive force.[29–33]

This motivates our exploration of shear wave speed estimation, a noninvasive elasticity technique that has minimal dependence on user interaction and greater ability to target the area of evaluation. A shear wave is a propagating disturbance of particle displacement generated in tissue produced by acoustic radiation force, and measuring its speed allows characterization of stiffness because propagation is faster in stiffer, and slower in softer, tissue.[34]

We studied shear wave speeds (SWS) in *ex vivo* cervices to investigate potential sources of biological variability and determine whether SWS estimates are sensitive enough to differentiate between ripened and unripened tissue. We found that SWS estimates may be promising for assessing cervical stiffness/softness. Ultimately, noninvasive quantitative methods to evaluate the cervix should facilitate comprehensive understanding of its microstructure and thus dictate novel approaches to the prediction and treatment of preterm birth.

METHODS

Tissue Acquisition

Hysterectomy specimens were collected from premenopausal subjects undergoing surgery for benign conditions not involving cervical pathology (n = 22). Exclusion criteria included a history of preterm birth, cervical surgery (including cerclage for preterm birth prevention), or collagen vascular disease. Pregnancy history, age, date of last menstrual period, and reason for hysterectomy were documented. Nine of the subjects were not experiencing uterine bleeding at the time of surgery (“unripened group”), 6 were either bleeding or experiencing significant dysmenorrhea and expecting menses near the time of surgery (“uterine bleeding group”), and 7 placed 400μg of misoprostol per vagina 10–12 hours prior to surgery to effect cervical softening (“misoprostol-ripened group”). Misoprostol is a prostaglandin used to ripen the cervix for induction of labor or gynecological procedures such as hysteroscopy, and our dose, route of administration, and timing of administration were based on clinical use of this agent in nonpregnant, premenopausal women.[35;36] All subjects provided informed consent, and all work was HIPAA compliant and approved by the IRBs at Intermountain Healthcare and the University of Wisconsin.

Immediately following excision, specimens were immersed in saline and brought to the pathology laboratory. Each sample was allowed to stabilize at room temperature prior to data acquisition (to exclude temperature as a source of potential variability between specimens). After the anatomy (anterior vs. posterior cervix) was identified by a gynecological pathologist, the sample was bivalved and secured to a piece of sound absorbing (SoAb) rubber with pins to prevent reverberations and minimize motion artifact. The pins were delicately placed along the contour of the cervix within the outer serosa to avoid distorting the tissue (Figure 1).

Data Acquisition

A Siemens Acuson S2000 ultrasound system (Siemens Healthcare, Ultrasound Business Unit, Mountain View, CA, USA) was used to acquire shear wave data via the Virtual Touch Tissue Quantification software package. Imaging parameters are summarized in Table 1.

Imaging was performed with a 9L4 linear array transducer that has a 38mm aperture. The transducer was securely attached to an x-y positioning stage, and aligned parallel to the endocervical canal. The focal depth was set to 3cm (close to the elevational focus) and the sample placed at the focus. Data were acquired along the length of the canal on both the anterior and posterior cervix (12:00 and 6:00) in 4–5 non-overlapping positions with a 5x5mm region of interest (ROI). Five replicate measurements were performed at each location and their average computed to improve estimate accuracy. The ROI for SWS estimation was placed at a fixed depth with its center midway through the thickness of the cervix from canal to outer edge (about 7mm deep -- the thickness for each half was 13.6±0.19 mm; mean±1 SD). This ROI placement excluded at least the first 2 mm of inner and outer boundaries to avoid unpredictable wave behavior at the outer edges of the sample.

Specialized software was used to acquire data from the S2000 for off-line data analysis with MATLAB (Mathworks, Natick, MA). Tissue displacement was estimated using Loupas' method on I-Q data.[37] This method allows for fast and accurate tracking of small displacements (< 10μm). A minimum correlation threshold of 0.98 was used to remove less reliable displacement estimates. The RANSAC algorithm, described by Wang et. al.,[38] was used for all wave speed estimates.

The mean cervical length was 2.79±0.38 cm. To standardize measurement locations among cervices of different lengths, the cervical canals were partitioned based on fractional distances from the internal os. The distal and proximal ends (external and internal os, respectively) were identified by a Maternal-Fetal Medicine subspecialist (HF) on the B-mode images, as illustrated in Figure 2(a), and measurements were made between these endpoints. Locations along the cervical canal were labeled as follows: 0–25% (Proximal), 26–44% (Mid-Proximal), 45–55% (Mid), 56–75% (Mid-Distal), and 76–100% (Distal). If a cervix was too short to allow 5 measurements, the mid measurement was considered as missing. In those cases, the average of the estimates obtained in the mid-distal and mid-proximal was used, effectively interpolating a "mid" estimate. The presence of nabothian cysts, as shown in Figure 2(b), disrupted shear wave propagation, so those locations were avoided. (These are easily identified with B-mode imaging thus will not be a hindrance to *in vivo* study.)

Statistical Analysis

The shear wave speed estimates were analyzed to evaluate (1) the spatial variability of SWS averaged over replicate measures as a function of position along the length of the canal, (2) the variability of SWS in the anterior vs. posterior cervix, and (3) the sensitivity of SWS to distinguish ripened from unripened cervical tissue.

We first determined whether the uterine bleeding (n=6) and misoprostol-ripened (n=7) groups could be combined into a single "ripened" group in order to increase the statistical power of comparisons between ripened and unripened tissue. To our knowledge, the concept that cervical microstructure is similarly affected whether prostaglandins are endogenous or exogenous has not been tested, although logic dictates this would be the case. Serum (endogenous) prostaglandins are elevated during uterine bleeding, especially with significant dysmenorrhea, and they cause cervical softening.[39–42] Similarly, exogenous prostaglandins soften the cervix and are used for various obstetrical and gynecological procedures including induction of labor,[43;44] surgical abortion,[35] or invasive procedures (e.g. hysteroscopy) involving traversing the internal cervical os to gain access to the uterine cavity.[35;36] As expected, these groups were not significantly different (see below), so they were combined and all remaining comparisons were performed between ripened (n=13) and unripened (n=9) tissue.

Statistical tests were performed with two-sample t-tests in MATLAB with a probability of equal means less than 0.05 (two-tailed) as the criterion for statistical significance. Tests performed on individual hypotheses (t-tests) can take only one variable into account at a time and we therefore corroborated significant findings with a linear mixed model. This provides a more robust comparison of individual results, and additionally incorporates multiple variables and hypotheses together in one model. This is advantageous because some variables may be related (covariant); in the cervix, these include anterior vs. posterior cervix measurements and level of increase in SWS vs. location (slope). Other advantages of this test include the ability to incorporate random effects (e.g. variability between cervices) and unequal sample sizes for each group. The linear mixed model tested for significant differences in SWS along the canal, anterior vs. posterior locations, and ripened vs. unripened tissue. The mixed model analysis was performed using R (Free Software Foundation's GNU project) with the 'nmle' package.

RESULTS

Categorization of Groups

Figure 3 shows summary results for SWS for the misoprostol-ripened and uterine bleeding groups at the mid location on the anterior and posterior sides. The interior lines display the medians, the edges of the boxes are the upper and lower quartiles (25th and 75th percentile) of the SWS estimates, and the bars ('whiskers') display the maxima and minima at each location [within 1.5*interquartile range (IQR)]. Outliers are specified as 1.5*IQR and are displayed as cross markers. The notch on the box plot represents the 95% confidence interval of the median. t-tests confirmed no significant difference between the misoprostol-ripened [SWS = 2.17±0.57 m/s (anterior), 2.67±0.64 m/s (posterior)] and uterine bleeding groups [SWS = 2.05±0.25 m/s (anterior), 2.70±0.51 m/s (posterior)]; corresponding p-values were 0.23 (anterior) and 0.45 (posterior). The linear mixed model did not find an interaction between ripening and slope in these groups (p=0.86), which reconfirmed the conclusion from the t-tests that these groups were appropriately combined.

Spatial Variability within the Cervix

Shear wave speed estimates demonstrated spatial variability both along the length of the cervix and within its anterior vs. posterior segments (Figure 4). The box plot shows the mean SWS estimates over replicate measures for each specimen at each location along the length of the cervix on both the anterior and posterior segments within each group. All groups had a significant slope in SWS ($p<0.0001$), an increase in SWS from distal to proximal end. A least-squares fit to the mean SWS at each position was computed to estimate the spatial gradient (change in stiffness along the canal). SWS gradients in the anterior sections were 0.86 and 0.31 $m \cdot s^{-1} cm^{-1}$ for the unripened and ripened groups, respectively. The corresponding gradients in the posterior sections followed the same trend, but were larger (1.22, 0.83 $m \cdot s^{-1} cm^{-1}$, respectively). Compared to the unripened group, the ripened group showed a lesser gradient (lesser increase in SWS) from distal to proximal locations along both the anterior and posterior side of the cervix, resulting in decreased variance within this group (Figure 4).

Sensitivity of SWS estimates to distinguish ripened from unripened tissue

Shear wave speed estimates effectively differentiated between unripened and ripened tissue. The largest difference in mean SWS between groups occurred proximally, and the least distally. A box plot demonstrating the sensitivity of SWS estimates to distinguish ripened from unripened cervical tissue is shown in Figure 5. SWS estimates from each specific location were combined (i.e. unripened anterior mid, unripened posterior mid, ripened anterior mid, and ripened posterior mid). The mean SWS for the anterior and posterior

segments of the unripened group were 3.45±0.95 m/s and 3.56±0.92 m/s respectively, and 2.11±0.45 m/s and 2.68±0.57 m/s for the ripened. t-tests at this location confirmed significant differences between ripened and unripened for both anterior and posterior measurements ($p < 0.001$). The linear mixed model supported and strengthened results of the individual t-tests, with p-values < 0.001 for ripened vs. unripened tissue.

DISCUSSION

Comprehensive quantitative assessment of the pregnant cervix is our ultimate goal, and will require calculation of elastic moduli. Eventually, this should be possible from shear wave speed measurement, but will demand sophisticated knowledge of the microstructure; wave propagation can be complicated by higher order material properties (i.e., viscosity and nonlinearity) and structural boundary conditions (e.g., within thin layers or at the surfaces of organs). Common assumptions that have been successfully applied to large organs such as liver are that the tissue is isotropic (same material properties in all spatial orientations), homogeneous, and semi-infinite (away from any boundaries).[45–47] These assumptions are inappropriate for the cervix, which is anisotropic, heterogeneous, and small (relative to the shear wavelengths [22±6 mm for unripened anterior mid location] generated with acoustic radiation force, complicating the relationship between wave propagation and underlying material properties). That said, appropriate interpretation of wave behavior should be possible if the inherent complexity of the cervix is respected. As an initial foray, we explored the ability of shear wave speeds (under the assumption of small areas, <5×5 mm, of homogeneity) to evaluate the extent of cervical biological variability in SWS and distinguish between ripened and unripened tissue.

We found significant, albeit consistent, variability within and between cervices. Our results demonstrate a monotonically increasing shear wave speed (a gradient in SWS) from the distal to proximal cervix (Figure 4). Proximal locations demonstrate the largest differences in mean SWS, and distal the least, which is interesting because ripening appears to initiate proximally.[8] We also found spatial variability within the anterior compared to posterior cervix; the SWS vs. location slope along the posterior cervix is significantly greater than anterior (the change in SWS along the posterior cervix is greater at each location compared to the anterior). Further, this difference is most marked in unripened tissue, suggesting that ripened cervices are more like each other than are unripened.

Our results also suggest that shear wave speed estimation effectively differentiates between ripened and unripened tissue; the significant difference in SWS found between the two groups is demonstrated by minimal overlap in IQRs shown in Figure 5. The SWS estimates increase from the distal to proximal cervix in both groups, with a greater increase observed in the unripened group (Figure 4). This suggests that ripening increases tissue homogeneity, a finding that is consistent with those from animal models.[18;24;28;48]

The important lesson from these experiments for transition to *in vivo* study is that biological variability, while fortunately predictable, is great enough even within a single cervix that sampling must be consistent among subjects in order to make meaningful comparisons.

We expect that the mid anterior or mid posterior location will be best for *in vivo* acquisition. Along the longitudinal axis, the proximal location demonstrates the greatest differences between groups, but the mid location also demonstrates clear differences, and seems safer; although our modeling indicates that shear wave imaging is safe, this type of imaging is relatively new. Shear waves have been explored in the liver for more than a decade, but only recently gained FDA approval. Until this has been extensively explored in obstetrics, it seems prudent to minimize potential risks from exposing the fetus to high intensity

ultrasound waves. Our technique allows directed acquisitions, and obtaining data from the mid location minimizes fetal exposure.

Further, that the anterior cervix displays a lesser SWS gradient than the posterior is important because as the slope increases, variance increases, thus increasing the possibility of measurement unreliability. Because of this, the most relevant information in the unripened nonpregnant cervix is gained from the anterior segment. Importantly however, this gradient difference is not as pronounced in ripened cervices and the pregnant cervix, which begins to soften soon after conception, should more closely resemble the nonpregnant ripened cervix. Therefore, although sampling clearly requires consistency because of spatial variability, whichever approach (anterior or posterior) is most feasible clinically should be equally acceptable.

The main limitations of this study relate to its *ex vivo* nature; namely, we bivalved the cervix and used a transducer unsuitable for *in vivo* scanning. Bivalving allowed efficient and comprehensive evaluation of the entire cervix, but likely changed its mechanical properties. The *in vivo* cervix is a thick-walled cylinder with a circumferential central layer of collagen, and disruption of such a layer changes mechanical properties. *In vitro* tissues also lack the turgor of perfused tissues, which may introduce a reduction in apparent tissue stiffness compared to the *in vivo* condition. Further, SWS estimates were made at room temperature, which also may introduce a bias in SWS estimates compared to *in vivo* tissues. However, the relevant finding is the overall pattern in spatial variability within the cervix, which should remain consistent.

Regarding the transducer, its advantage is its large size (aperture 38 mm), but that also makes it unsuitable for endocavity scanning. The prototype transducer we are exploring for i*n vivo* use[50] is 3 mm in diameter. It has a 14mm side-firing array capable of generating high intensity pulses for shear wave techniques, and SWS estimates from the two transducers are comparable (data submitted elsewhere). The shorter lateral tracking range this small aperture creates is not a problem for a low number of acquisitions (a single acquisition takes approximately 1 minute), but would have been a problem for this study because the large number of replicate SWS measurements required would have impractically increasing acquisition time.

In summary, shear wave speed estimation, which should ultimately allow calculation of elastic moduli, may be an excellent component of targeted and comprehensive exploration of the *in vivo* cervix. The considerable spatial variability within the cervix dictates that acquisition location should be standardized, but with appropriate comparisons, SWS estimates effectively distinguish between ripened and unripened tissue. We do not expect significant obstacles to adapting our approach to the *in vivo* cervix, and in fact preliminary results are encouraging. Quantitative methods to assess cervical microstructural changes during pregnancy should facilitate elucidation of associated molecular mechanisms, which should finally reveal novel approaches to the prevention and prediction of preterm birth.

Acknowledgments

This work was supported by NIH Grants R21HD061896, R21HD063031 and R01HD072077 from the Eunice Kennedy Shriver National Institute of Child Health and Human Development. The authors would also like to recognize Dr. Michael Wang for providing the RANSAC code, Dr. Paul Urie and Deanna Staker, PA-C in the Pathology Department at Utah Valley Regional Medical Center for their invaluable assistance, and the obstetrician-gynecologists at Utah Valley Regional for providing access to their patients for this study. We are also grateful to Siemens Healthcare Ultrasound division for equipment loan and technical support.

References

1. Beck S, Wojdyla D, Say L, Betran AP, Merialdi M, Requejo JH, Rubens C, Menon R, VanLook PF. The worldwide incidence of preterm birth: a systematic review of maternal mortality and morbidity. Bull World Health Organ. 2010; 88:31–38. [PubMed: 20428351]
2. Norman JE, Shennan AH. Prevention of preterm birth – why can't we do any better? Lancet. 2013; 19:184–185. [PubMed: 23158880]
3. Romero R. Prevention of spontaneous preterm birth: The role of sonographic cervical length in identifying patients who may benefit from progesterone treatment. Ultrasound Obstet Gynecol. 2007; 30:675–686. [PubMed: 17899585]
4. Romero R. Vaginal progesterone to reduce the rate of preterm birth and neonatal morbidity: a solution at last. Womens Health (Lond Engl). 2011; 7:501–504. [PubMed: 21879816]
5. Gravett MC, Rubens CE, Nunes TM. GAPPS Review Group. Global report on preterm birth and stillbirth (2 of 7): discovery science. BMC Pregnancy Childbirth. 2013; 10 (Supp1):S2. [PubMed: 20233383]
6. Menon R, Dunlop AL, Kramer MR, Fortunato SJ, Hogue CJ. An overview of racial disparities in preterm birth rates: caused by infection or inflammatory response? Acta Obstet Gynecol Scand. 2011; 90:1325–1331. [PubMed: 21615712]
7. Muglia LJ, Katz M. The enigma of spontaneous preterm birth. New Engl J Med. 2013; 362:529–535. [PubMed: 20147718]
8. Word RA, Li XH, Hnat M, Carrick K. Dynamics of cervical remodeling during pregnancy and parturition: Mechanisms and current concepts. Semin Reprod Med. 2007; 25:69–79. [PubMed: 17205425]
9. Uldbjerg N, Malmström A, Ekman G, Sheehan J, Ulmsten U, Wingerup L. Isolation and characterization of dermatan sulphate proteoglycan from human uterine cervix. Biochem J. 1983; 209:497–503. [PubMed: 6847631]
10. Danforth D. The morphology of the human cervix. Clin Obstet Gynecol. 1983; 26:7–13. [PubMed: 6839572]
11. Parry DA. The molecular and fibrillar structure of collagen and its relationship to the mechanical properties of connective tissue. Biophys Chem. 1988; 29:195–209. [PubMed: 3282560]
12. Kleissl HP, van der Rest M, Naftolin F, Glorieux FH, de Leon A. Collagen changes in human uterine cervix at parturition. Am J Obstet Gynecol. 1978; 130:748–753. [PubMed: 637097]
13. Theobald PW, Rath W, Kühnle H, Kuhn W. Histological and electron-microscopic examinations of collageneous connective tissue of the non-pregnant cervix, the pregnant cervix, and the pregnant prostaglandin-treated cervix. Arch Gynecol. 1982; 231:241–245. [PubMed: 7125705]
14. Rechberger T, Uldbjerg N, Oxlund H. Connective tissue changes in the cervix during normal-pregnancy and pregnancy complicated by cervical incompetence. Obstet Gynecol. 1988; 71:563–567. [PubMed: 3353047]
15. Rechberger T, Abramson SR, Woessner JF Jr. Onapristone and prostaglandin E2 induction of delivery in the rat in rate pregnancy: A model for the analysis of cervical softening. Am J Obstet Gynecol. 1996; 175:719–723. [PubMed: 8828440]
16. Read CP, Word RA, Ruscheinsky MA, Timmons BC, Mahendroo MS. Cervical remodeling during pregnancy and parturition: characterization of the softening phase in mice. Reproduction. 2007; 134:327–340. [PubMed: 17660242]
17. Timmons B, Akins M, Mahendroo M. Cervical remodeling during pregnancy and parturition. Trends Endocrinol Metab. 2010; 21:353–361. [PubMed: 20172738]
18. Feltovich H, Ji H, Janowski JW, Delance NC, Moran CC, Chien EK. The effects of nonselective PGE2 receptor agonists on cervical tensile strength and cervical collagen content and structure. Am J Obstet Gynecol. 2006; 92:753–760.
19. Keeler SM, Rust OA, Kiefer DG, Prutsman WJ, Proudfit CL, Naftolin F. Controlled fine needle biopsy of the uterine cervix during pregnancy. Reprod Sci. 2011; 18:737–742. [PubMed: 21421896]
20. Dubrauszky V, Schwalm H, Fleischer M. Fibre system of connective tissue in childbearing age, menopause, and pregnancy. Archiv Gynakol. 1971; 210:276–292.

21. Hukins DW, Aspden RM. Composition and properties of connective tissues. Trends Biochem Sci. 1985; 10:260–264.
22. Aspden RM. Collagen organization in the cervix and its relation to mechanical function. Coll Relat Res. 1988; 8:103–112. [PubMed: 3378391]
23. Weiss S, Jaermann T, Schmid P, Staempfli P, Boesiger P, Niederer P, Caduff R, Bajka M. Three-dimensional fiber architecture of the nonpregnant human uterus determined *ex vivo* using magnetic resonance diffusion tensor imaging. Anat Rec A Discov Mol Cell Evol Biol. 2006; 288:84–90. [PubMed: 16345078]
24. Myers K, Socrate S, Tzeranis D, House M. Changes in the biochemical constituents and morphologic appearance of the human cervical stroma during pregnancy. Eur J Obstet Gynecol Reprod Biol. 2009; 144:S82. [PubMed: 19303693]
25. Breeveld-Dwarkasing VN, de Boer-Brouwer M, te Koppele JM, Bank RA, van der Weijden GC, Taverne MA, van Dissel-Emiliani FM. Regional differences in water content, collagen content, and collagen degradation in the cervix of nonpregnant cows. Bio Reprod. 2003; 69:1600–1607. [PubMed: 12855607]
26. Breeveld-Dwarkasing VN, te Koppele JM, Bank RA, van der Weifden GC, Taverne MA, van Dissel-Emiliani FM. Changes in water content, collagen degradation, collagen content and concentration on repeat biopsies of the cervix of pregnant cows. Biol Reprod. 2003; 69:1608–1614. [PubMed: 12855606]
27. Akins ML, Luby-Phelps K, Mahendroo M. Second harmonic generation imaging as a potential tool for staging pregnancy and predicting preterm birth. J Biomed Opt. 2010; 15:026020. [PubMed: 20459265]
28. Feltovich H, Hall TJ, Berghella V. Beyond cervical length: emerging technologies for assessing the pregnant cervix. Am J Obstet Gynecol. 2012; 207:345–354. [PubMed: 22717270]
29. Swiatkowska-Freund M, Preis L. Elastography of the uterine cervix: implications for success of induction of labor. Ultrasound Obstet Gynecol. 2011; 38:52–56. [PubMed: 21484905]
30. Molina FM, Gómez LF, Florido J, Padilla MC, Nicolaides KH. Quantification of cervical elastography: a reproducibility study. Ultrasound Obstet Gynecol. 2012; 39:685–689. [PubMed: 22173854]
31. Hernandez-Andrade E, Hassan SS, Ahn H, Korzeniewski SJ, Yeo L, Chaiworapongsa T, Romero R. Evaluation of cervical stiffness during pregnancy using semiquantitative ultrasound elastography. Ultrasound Obstet Gynecol. 2013; 41:152–161. [PubMed: 23151941]
32. Fruscalzo A, Steinhard J, Londero AP, Fröhlich C, Bijnens B, Klockenbusch W, Schmitz R. Reliability of quantitative elastography of the uterine cervix in at-term pregnancies. J Perinat Med. 2013; 7:1–7.
33. Feltovich H, Hall TJ. Quantitative imaging of the cervix: setting the bar. Ultrasound Obstet Gynecol. 2013; 41:121–128. [PubMed: 23371343]
34. Doherty JR, Trahey GE, Nightingale KR, Palmeri ML. Acoustic radiation force elasticity imaging in diagnostic ultrasound. IEEE Trans Ultrason Ferroelectr Freq Control. 2013; 60:685–701. [PubMed: 23549529]
35. Allen R, O'Brien BM. Uses of misoprostol in obstetrics and gynecology. Rev Obstet Gynecol. 2009; 2:159–168. [PubMed: 19826573]
36. Crane JM, Healey S. Use of misoprostol before hysteroscopy: a systematic review. J Obstet Gynaecol Can. 2006; 28:373–379. [PubMed: 16768880]
37. Pinton GF, Dahl JJ, Trahey GE. Rapid tracking of small displacements with ultrasound. IEEE Trans Ultrason Ferroelectr Freq Control. 2006; 53:1103–1117. [PubMed: 16846143]
38. Wang MH, Palmeri ML, Rotemberg VM, Rouze NC, Nightingale KR. Improving the robustness of time-of-flight based shear wave speed reconstruction methods using RANSAC in human liver *in vivo*. Ultrasound Med Biol. 2010; 36:802–813. [PubMed: 20381950]
39. Clark K, Myatt L. Prostaglandins and the reproductive cycle. Gynecology and Obstetrics. 2004; 5 CD-ROM.
40. Pulkkinen MO, Henzl MR, Csapo AI. The effect of naproxen sodium on the intrauterine pressure and menstrual pain of dysmenorrheic patients. Prostaglandins. 1978; 15:543–550. [PubMed: 351717]

41. Chain WY, Dawood MY. Prostaglandin levels in menstrual fluid of nondysmenorrheic and dysmenorrheic subjects with and without oral contraceptive on ibuprofen therapy. Adv Prostaglandin Thromboxane Res. 1980; 8:1443–1447. [PubMed: 7376995]

42. Pickles VR, Hall WJ, Best FA, Smith GN. Prostaglandins in endometrium and menstrual fluid from normal and dysmenorrhoiec subjects. J Obstet Gynaecol Br Commonw. 1965; 72:185–192. [PubMed: 14273094]

43. Kelly AJ, Malik S, Smith L, Kavanagh J, Thomas J. Vaginal prostaglandin (pge2 and pgf2a) for induction of labour at term. Cochrane Database Syst Rev. 2009; 7:CD003101. [PubMed: 19821301]

44. Hofmeyr GJ, Gülmezoglu AM, Pileggi C. Vaginal misoprostol for cervical ripening and induction of labour. Cochrane Database Syst Rev. 2010; 6:CD000941. [PubMed: 20927722]

45. Bouchard RR, Dahl JJ, Hsu SJ, Palmeri ML, Trahey GE. Image quality, tissue heating, and frame rate trade-offs in acoustic radiation force impulse imaging. IEEE Trans Ultrason Ferroelectr Freq Control. 2009; 56:63–76. [PubMed: 19213633]

46. Sharma AC, Soo MS, Trahey GE, Nightingale KR. Acoustic radiation force impulse imaging of in vivo breast masses. IEEE Ultrason Symp. 2004; 1:728–731.

47. Palmeri ML, Wang MH, Rouze NC, Abdelmalek MF, Guy CD, Moser B, Diehl AM, Nightingale KR. Noninvasive evaluation of hepatic fibrosis using acoustic radiation force-based shear stiffness in patients with nonalcoholic fatty liver disease. J Hepatol. 2011; 55:666–672. [PubMed: 21256907]

48. Clark K, Ji H, Feltovich H, Janowski J, Carroll C, Chien EK. Mifepristone-induced cervical ripening: structural, biochemical, and molecular events. Am J Obstet Gynecol. 2006; 194:1391–1398. [PubMed: 16647925]

49. Myers KM, Paskaleva AP, House M, Socrate S. Mechanical and biochemical properties of human cervical tissue. Acta Biomater. 2008; 4:104–116. [PubMed: 17904431]

50. Feltovich H, Nam K, Hall TJ. Quantitative ultrasound assessment of cervical microstructure. Ultrason Imaging. 2010; 32:131–142. [PubMed: 20718243]

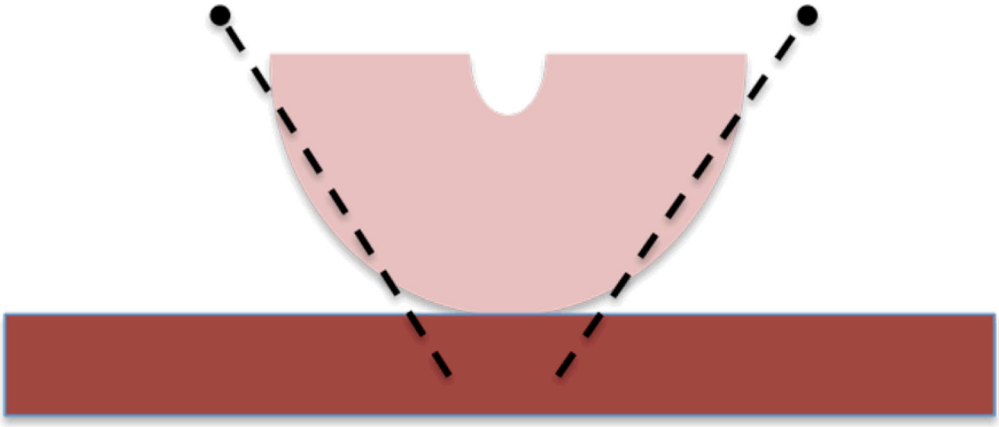

Figure 1.
Schematic showing distal view of cervix on top of rectangular piece of SoAb. The pins were placed delicately along the contours of the outer serosa of the cervix to prevent distortion of the tissue.

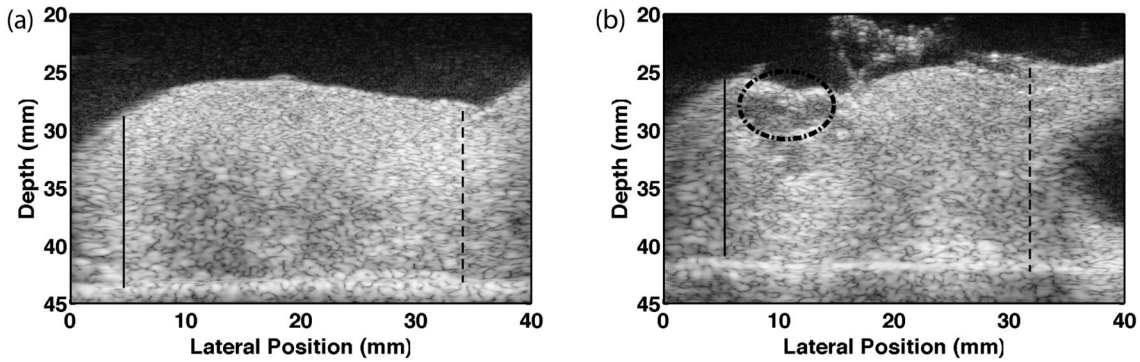

Figure 2.

B-mode images of half of a bivalved cervix sample. The endocervical canal is located at the top, the distal end is on the left and proximal end/uterus is on the right. The bright line on the bottom is the SoAb rubber interface. The **solid** lines mark the distal end (external os) and the **dashed lines** the proximal end (internal os). These locations were verified by HF (the Maternal Fetal Medicine subspecialist co-author). Measurements were made between these endpoints. The image on the right shows a sample containing cysts (**dashed** circle), and the black region is a uterine fibroid. These areas were avoided during measurements.

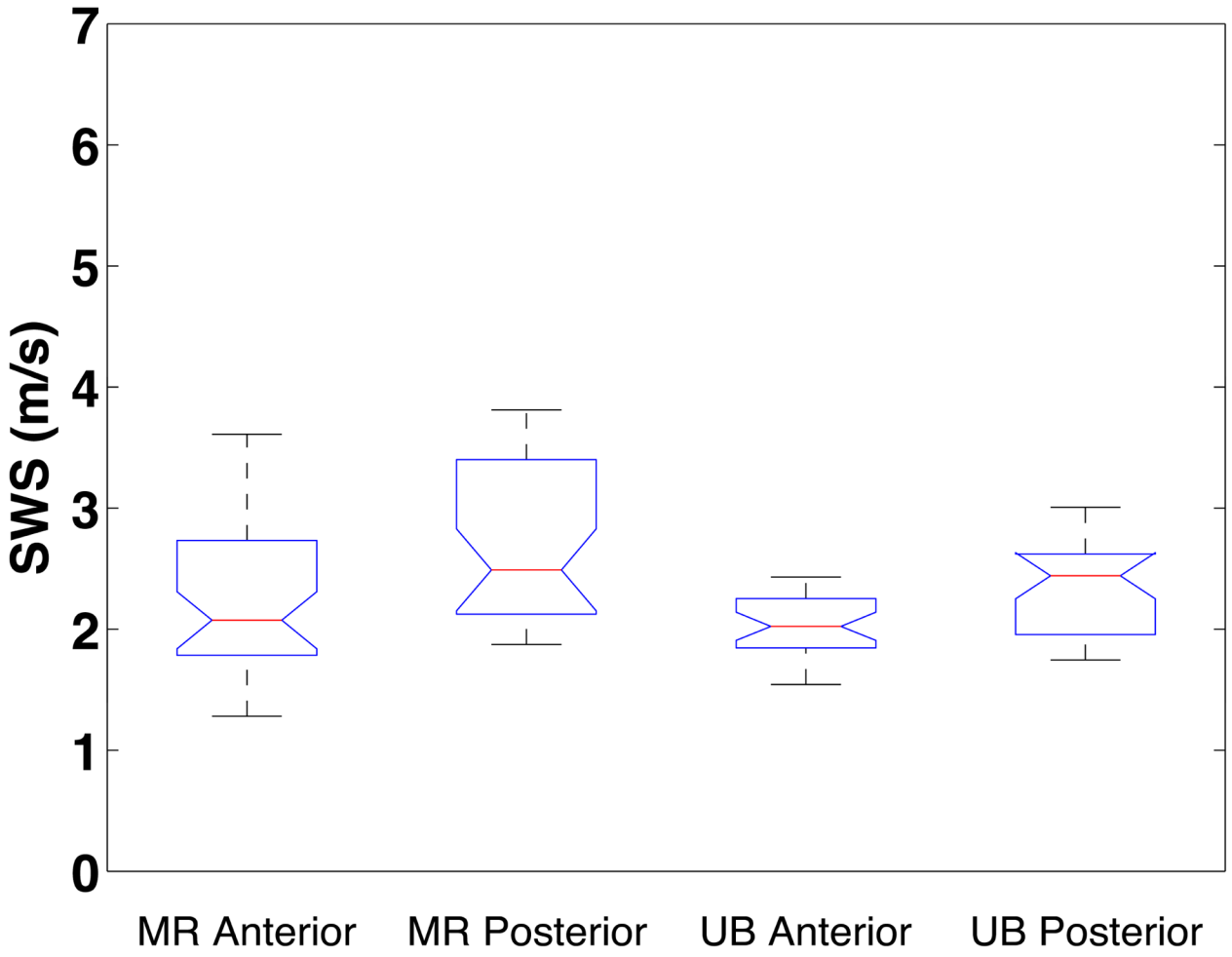

Figure 3.
Box plots of **mid** location **SWS** vs. type of ripening and anterior/posterior. Misoprostol ripened group (MR) Anterior and Posterior are shown on the left. The right boxes show the uterine bleeding (UB) group Anterior and Posterior, respectively.

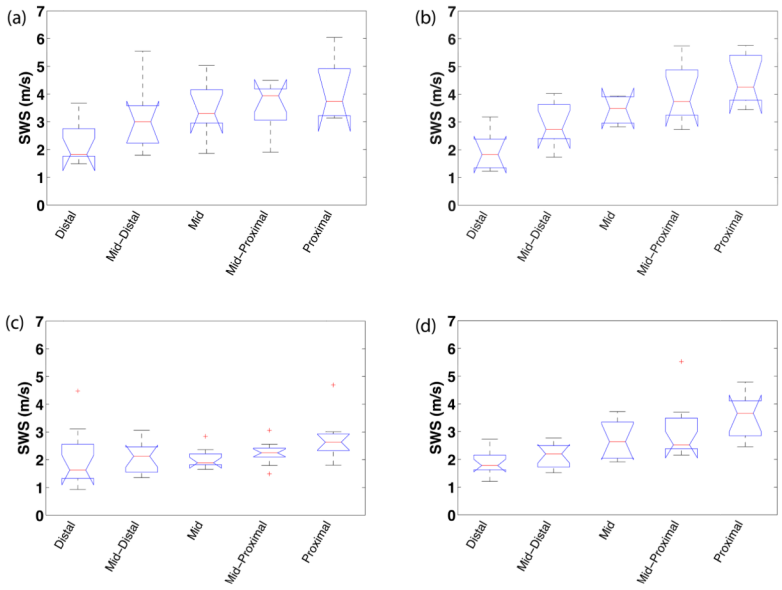

Figure 4.

Box plots of mean SWS from each sample vs. cervical canal location for each group and cervix half: unripened (a–b) and ripened (c–d); anterior **(a,c)** and posterior **(b,d)** slices. The boxes represent interquartile range (IQR), interior line is median, whiskers are maxima and minima within 1.5*IQR, and cross markers show outliers beyond the 1.5*IQR.

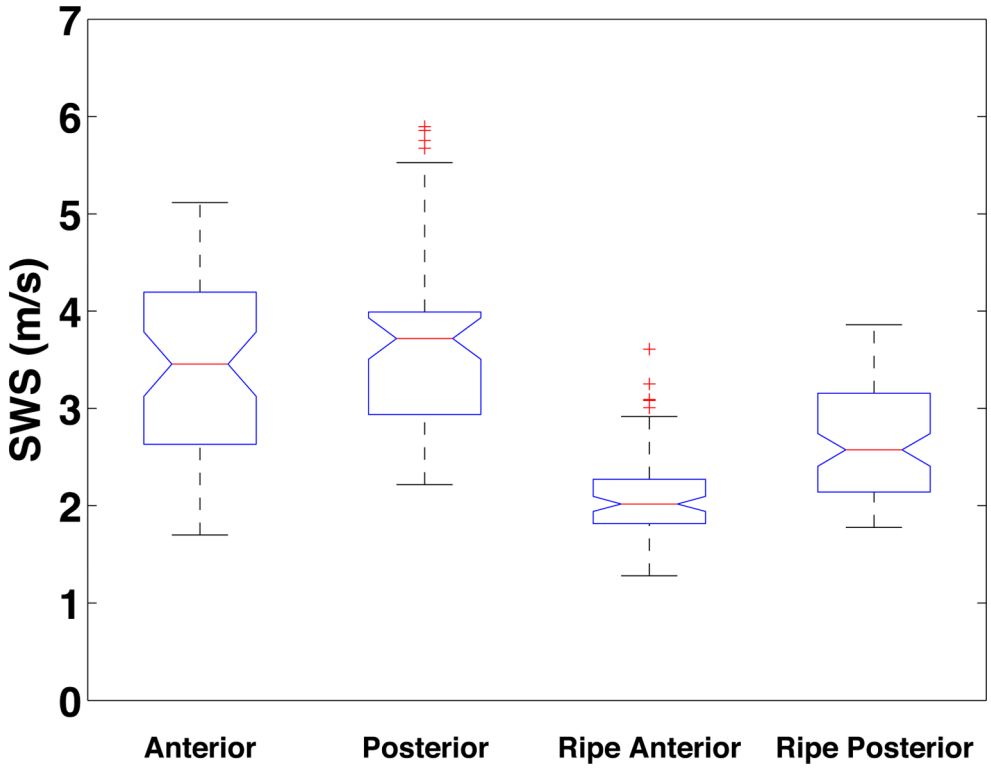

Figure 5.
Box plot of **SWS** in the **mid** location for each group: Unripened Anterior, Unripened Posterior, Ripened Anterior, Ripened Posterior from left to right, respectively.

Table 1

Summary of acoustic parameters. F-number is defined as the ratio of focal depth to active aperture width and describes the imaging system focal properties. These parameters are necessary for generation of acoustic force and accurate displacement tracking for shear wave estimation.

Parameter	Value
Probe	9L4
Push Frequency (MHz)	4
Track Frequency (MHz)	6.15
Push Cycles	400
Pulse Duration	100μs
Track Pulse Repetition Frequency	9259Hz
Push F-number	1.5
Track F-number	1.5
Push focal depth	3cm
Elevation focus	3.8cm
MI	1.9